ETH zürich

ETH Library

Random Lasing with Systematic Threshold Behavior in Films of CdSe/CdS Core/Thick-Shell Colloidal Quantum Dots

Journal Article

Author(s):
Gollner, Claudia; Ziegler, Johannes; Protesescu, Loredana; Dirin, Dmitry N.; Lechner, Rainer T.; Fritz-Popovski, Gerhard; Sytnyk, Mykhailo; Yakunin, Sergii; Rotter, Stefan; Yousefi Amin, Amir A.; Vidal, Cynthia; Hrelescu, Calin; Klar, Thomas A.; Kovalenko, Maksym V.; Heiss, Wolfgang

Publication date:
2015-09

Permanent link:
https://doi.org/10.3929/ethz-b-000106319

Rights / license:
In Copyright - Non-Commercial Use Permitted

Originally published in:
ACS Nano 9(10), https://doi.org/10.1021/acsnano.5b02739

This page was generated automatically upon download from the ETH Zurich Research Collection.
For more information, please consult the Terms of use.

Random Lasing with Systematic Threshold Behavior in Films of CdSe/CdS Core/Thick-Shell Colloidal Quantum Dots

*Claudia Gollner,[1] Johannes Ziegler,[2] Loredana Protesescu,[3,4] Dmitry N. Dirin,[3,4] Mykhailo Sytnyk,[1] Sergii Yakunin,[1,3,4] Stefan Rotter,[5] Cynthia Vidal,[2] Calin Hrelescu,[2] Thomas A. Klar,[2] Maksym Kovalenko,[3,4] and Wolfgang Heiss[1,6,7]**

[1]Institute of Semiconductor and Solid State Physics, Johannes Kepler University Linz, Altenberger Straße 69, 4040 Linz, Austria;

[2]Institute of Applied Physics, Johannes Kepler University Linz, Altenberger Straße 69, 4040 Linz, Austria;

[3]Department of Chemistry and Applied Biosciences, ETH Zürich, Vladimir-Prelog-Weg 1, 8093 Zürich, Switzerland;

[4]Empa-Swiss Federal Laboratories for Materials Science and Technology, Überlandstrasse 129, 8600 Dübendorf, Switzerland;

[5]Institute for Theoretical Physics, Vienna University of Technology, Wiedner Hauptstraße 8-10/136, 1040 Vienna, Austria;

[6]Materials for Electronics and Energy Technology (i-MEET), Friedrich-Alexander-Universität Erlangen-Nürnberg, Martensstraße 7, 91058 Erlangen, Germany;

[7]Energie Campus Nürnberg (EnCN), Fürther Straße 250, 90429 Nürnberg, Germany.

*corresponding Author: Wolfgang.Heiss@fau.de

KEYWORDS giant shell quantum dots, successive ion layer adsorption and reaction, random lasing, exciton-exciton interactions, plasmonics

ABSTRACT While over the last years the syntheses of colloidal quantum dots (CQDs) with core/shell structures were continuously improved to obtain highly efficient emission, it has remained a challenge to use them as active materials in laser devices. Here, we report on a successful demonstration of random lasing at room temperature in films of CdSe/CdS CQDs with different core/shell band alignments and extra thick shells. Even though the lasing process is based on random scattering, we find systematic dependencies of the laser thresholds on film morphology and excitation spot size. This systematics suggests that random lasing experiments are a valuable tool for testing nanocrystal materials, providing a direct and simple feedback for the further development of colloidal gain materials towards lasing in continuous wave operation.

INTRODUCTION

Colloidal quantum dots (CQDs) based on CdSe nanocrystals covered by protective inorganic shells are an attractive material system due to their simple fabrication in solution, their size adjustable optical properties, and their high environmental stability.[1-11] They also exhibit a preeminent photoluminescence (PL) quantum yield,[12-14] which suggested their use as nano-photonic light sources, e.g., as fluorescence markers for bio-labeling[15-19] as active material in quantum dot based light emitting diodes[20-25] or to study the emission of single photons[26-28] in quantum-optical systems. In contrast to these applications based on spontaneous emission, CQDs exhibit severe drawbacks with respect to bulk semiconductors or nanoparticles of higher dimensionality (rods[29] and platelets[30-31]) in laser devices. This is because in CQDs the desired population inversion effectively dissipates by non-radiative Auger recombination, whose efficiency increases rapidly with decreasing dot radius r by $1/r^3$, and competes with the stimulated emission.[32-34] Thus, stimulated emission from CQDs is observed solely under intense, pulsed laser excitation. Contradictory statements are reported, concerning the optimum density of the CQDs in the gain material. While initial gain measurements were presented in dense CQD films,[35] laser emission has also been reported subsequently in droplets of diluted CQD solutions,[36] or for a small number of CQDs, dispersed on the surface of silica based, toroidal micro-resonators.[37] Interestingly, for the latter case record threshold energy densities have been achieved, which are about three orders of magnitude lower than those reported for the initial lasing experiments, performed on densely filled glass capillaries (at 77 K), used as ring resonators (see Table S1), even though similar CQD materials have been used. Significantly improved laser performance has been achieved by making use of especially designed core/shell nano-architectures with engineered exciton-exciton interactions, which were used to circumvent

Auger recombination in CQDs due to exciton-exciton repulsion.[38] Thus, laser thresholds depend on a combination of material related as well as CQD specific parameters, which aggravates any systematic screening for optimized nanocrystal-based laser materials by measuring thresholds of individual laser devices.

Besides conventional lasers with judiciously engineered optical resonators, also random lasers recently attracted a lot of attention, due to a set of appealing properties.[39-52] In random lasers, the optical feedback is provided by disorder-induced light scattering, for instance achieved by mixing scattering particles into a laser-gain material.[43] In such mixtures, the light confinement is realized by the disorder scattering. The multiple scattering events involved in this process give rise to highly complex modes which can nevertheless result in narrow emission peaks.[43] Modal interactions through the gain medium in such lasers can be extremely strong, leading to an uniformly spaced frequency spectrum.[44] Random lasing is expected to have advantages in comparison to conventional lasing in illumination purposes as, e. g., for speckle free images[50] using suitable designed random lasers with low spatial coherence. To control random lasers is a challenging problem on which, however, much progress has been reported, recently.[39-41, 45, 47, 53] Quantum dot based random lasing has already been observed in CdSe/ZnS core-shell CQDs, by depositing them on glass substrates with roughened grooves.[54] In this case the rough surfaces of the grooves are considered to be important for enabling laser feedback, and a threshold fluence of 25 mJ/cm^2 is reported.

In this work, we present a systematic and thorough investigation of CQD-based random lasing, while the earlier report[54] only provides principle evidence that random lasing in CQDs is feasible. Our samples are uniform films of CdSe/CdS CQDs on planar glass substrates. By scanning the sample and recording laser thresholds at various positions, we find a systematic and

reproducible relation between laser threshold and sample morphology. We measure the stray light from the films under microscopic dark field illumination to characterize the topography of the films. The experiments were performed for core-shell CQDs with attractive as well as with repulsive exciton-exciton interactions, providing consistent dependencies and higher thresholds for the CQDs of the repulsive type. This is a nontrivial finding, because in case of repulsive interaction, two effects compete: First, the repulsive force decreases Auger recombination, which should lower the threshold. Second, however, repulsive interaction leads to a blue shift of the lasing frequency, leading in turn to a spectral overlap with the CQD absorption. These results show that the systematic investigation of random lasing represents a powerful tool to evaluate and select CQD materials, which is probably better suited than the investigation of conventional lasing for which the thresholds are greatly affected by the choice of the used optical resonators.

RESULTS AND DISCUSSION

To achieve population inversion, being a prerequisite for the occurrence of laser emission, highly intense optical excitation is usually required,[35-36] which eventually causes damage to the nanocrystal materials. Therefore, in this study, highly emissive CdSe/CdS core shell nanocrystals were used, which are protected by extra thick shells. In particular, three types were investigated, namely (i) CdSe nanocrystals with zinc- blende structure and a shell of CdS grown by 'successive ion layer adsorption and reaction' (SILAR),[4] whereby 8 layers were adsorbed (henceforth called SILAR I sample), (ii) CdSe nanocrystals as before, but with 12 monolayers of CdS (called SILAR II) and (iii), CdSe nanocrystals with wurtzite structure and a high-quality so called Giant Shell of CdS, grown by the process described by Chen *et al.*[8] (for the synthesis see methods section and for microscope images see Figures S1). Here, both shell types were found to

provide high environmental stability, so that all samples could be reproducibly measured while kept and stored in air. The CQDs SILAR I and SILAR II have a core diameter of 3.55 nm and 3.60 nm, respectively, and display different shell thicknesses, namely 4.66 nm and 6.98 nm. These CQDs exhibit PL quantum yields of 44% and 53% in solution. For the Giant Shell CQDs, an even higher quantum yield of 69% was found, which is typical for high quality core/shell nanocrystal quantum dot materials.[2-3, 8] As device structures for lasing experiments, thin nanocrystal films were deposited by doctor blade casting on glass substrates, which then act as two-dimensional optical waveguides. To evidence the lasing capability of both, the nanocrystal materials as well as the films with thicknesses in the order of 1-2μm, we first measured amplified spontaneous emission (ASE) in a stripe geometry.[55] Under pulsed excitation (532 nm, ~8 ps pulses), all studied CdSe/CdS CQDs exhibited a PL maximum close to 630 nm. Above a certain threshold, an additional narrow peak evolved, caused by amplified spontaneous emission (Figure 1(a-c)). While the PL is associated to single-exciton (X) emission, the ASE is associated to emission from biexcitons (XX), evidencing a population inversion and gain in CQDs.[35] The ASE peak of the sample SILAR I is red-shifted with respect to the PL center by 43.5 meV (Fig. 1a). This red-shift indicates a positive biexciton binding energy, due to attractive exciton-exciton interactions, as is typically found in core/shell CQDs with a type-I band alignment.[38] In sample SILAR II the ASE is found close to the center of the excitonic PL peak (Fig. 1b), which is attributed to a biexciton with vanishing binding energy, indicative of a quasi type II band alignment between core and shell material. Alternatively, the ASE peak on top of the PL maximum could also be ascribed to optical gain from the single-excitons. In this case, according to Klimov *et al.*,[38] a second ASE peak should appear at higher pump intensities due to biexcitons. In our experiments, however, even up to the maximum available pump energies of

0,5 mJ, no such second peak could be observed. In addition, the threshold intensity for ASE for this sample was found close to that of SILAR I, for which the assignment of the ASE peak to biexcitons is not in question. Furthermore, transient pump-probe experiments confirmed this assignment, by exhibiting a bi-exponential decay, due to a fast XX-decay and a much slower X recombination (Figure S2). Essentially, this interpretation is in agreement with Cihan *et al.*[56] In contrast to the SILAR samples, the Giant Shell sample (Figure 1c) exhibits a blue shifted ASE peak. This blue shifted ASE results from a repulsive exciton-exciton interaction, which is known to occur in core/shell CQDs with a type-II band alignment. The type II is considered to be beneficial with respect to Auger recombination, whose rate is reported to be reduced as compared to that in type I core/shell CQDs[57] (due to the charge separation between the core and shell material). Furthermore, the radiative lifetime of the single exciton should be prolonged, due to the reduced overlap between electron and hole wavefunctions. Indeed, in the Giant Shell sample the X-decay time is up to three times longer than in the SILAR samples (τ_X=19 ns for Giant Shell, 13.8 ns for Silar II, and 4.5 ns for Silar I, Figure S3). Such an increase of lifetime for increasing charge separation is similar to those previously reported for type I/type II CQDs of CdTe/CdS or CdTe/CdSe[58] or of CdTe/ZnS.[59]

Random lasing supported by plasmonic gold nanostars. The conventional approach towards random lasing is to immerse an arrangement of scattering particles into an optical gain material where the particles provide the required optical feedback, by causing multiple scattering events. Thus in a first attempt to achieve random lasing in CQD films, we made use of gold nanoparticles, integrated into the wave-guiding SILAR I CQD film, similar as has been reported previously.[60-61] To efficiently scatter the emission from the CQDs, the plasmon resonance of the gold nanoparticles needs to overlap with the CQD PL spectrum. Thus we have chosen star

shaped gold nanoparticles exhibiting a broad extinction maximum at 647 nm due to Rayleigh scattering[62] close to the CQD's PL peak (Figure 2a). The ~100 nm large gold nanostars (Figure 2c) were deposited from a dilute solution on a glass substrate, prior to the deposition of the CQD film, to obtain a waveguide containing a random distribution of plasmonic scattering centers. These centers are clearly observed in the optical microscope image in Figure 2b, obtained under dark field illumination. The CQD-gold nanostars composite film was excited by 1.3 ns laser pulses (532 nm, 100 Hz repetition rate) which were only moderately focused to a 200 μm diameter spot, to overcome a critical minimal gain volume.[43] The emission spectra, collected in backscattering geometry, exhibited unmistakable signatures of lasing behavior (Figure 2d). Narrow emission peaks appeared above a threshold intensity of 16.6 mJ/cm². With increasing intensity, the number of spectrally narrow laser modes increased and for a pump intensity of 31 mJ/cm², a rather symmetrical emission spectrum was observed, with a spectral distance between the individual lasing modes of ~0.7-0.9 nm and linewidths around 0.3 nm. The threshold behavior is further evidenced by the kink in the dependence of the peak intensity as a function of the pumping intensity (the inset of Figure 2d shows the maximum amplitude of the PL spectra). Therefore, we conclude that our CQD films clearly show the hallmarks of a random laser.

Random Lasing from pure CQD films. The random lasing described above can be attributed to the feedback caused by multiple scattering events at the incorporated plasmonic gold nanostars. However, we also observed random lasing in CQD films that do not contain any additional scattering centers. In this case, an even 25 times higher repetition rate of the excitation laser (2.5 kHz instead of 100 Hz) could be used, because the CdSe/CdS core/shell nanocrystals turned out to be substantially more stable under intense laser excitation than the gold nanostars. The latter showed the tendency to melt when more energy is deposited, due to the higher

repetition rates. Surprisingly, the pure CQD films exhibited also a clear lasing behavior, as is exemplarily shown in Figures S4 for SILAR I CQDS and in Figure 3a for SILAR II CQDs. For both cases the threshold intensity was similar and lower as compared to the value achieved with gold nanoparticle scattering. In Figure 3a the lasing threshold is reached at a pump intensity of 2.2 mJ/cm², above which a first narrow mode appears at a wavelength of 642 nm, right in the center of the ASE spectrum of this sample (Figure 1b). When the pump intensity is further increased, additional lasing modes emerge, whose line widths (< 0.2 nm) were limited by the spectrometer resolution. The modes were rather stable and their shift from subsequently taken spectra was in the range of their line width. This is shown in Figure S5a, exhibiting spectra collected for single excitation pulses (the data shown in Figures 2 and 3 are integrated over many excitation pulses). However, strong mode competition is observed - with increasing pump power, some modes became suppressed whereas others became more pronounced (Figures 3). This can be ascribed to both, the spectral and the spatial overlap of random laser modes. The multi-mode spectrum observed in our samples also shows variations from shot to shot, in correspondence to previous observations along the same lines.[63] The sensitivity with respect to a slight modification in the pump is clearly evidenced by the set of spectra measured for single pulse excitations (see Figure S5a). Further, the spacing between the modes was similarly pronounced as in the case of the nanostar-supported random lasing (Fig. 2d, Figure 5a)

In contrast, the random lasing in a film of the Giant Shell sample shows a different behavior (Figure 3b). In this case, just above the lasing threshold, the spectra do not exhibit individual narrow peaks, but rather form a shape like the ones in the ASE measurements of the same sample (Fig. 1c). Only at excitation intensities substantially higher than the threshold, individual modes appear in the spectra (which are integrated over many excitation pulses). Also the spectra

collected after single pulse excitation show a slightly different behavior than that for the SILAR I and II samples, in that the spectral positions of some of the modes vary from pulse to pulse, and the mode distances are rather irregular (Figure S5b). We attribute the spectral behavior of the Giant Shell sample showing the ASE like laser spectra to a lack of spatial coherence, which indicates the origin of scattering to be a different one than that of the SILAR I and II samples. To unravel these differences, the surface morphology of the films was investigated by atomic force microscopy (AFM) (see Figure 4) and indeed, substantial different film forming properties were observed for the SILAR samples and the Giant Shell sample. While the Giant Shell sample exhibited a substantial film roughness and showed distinct pits with varying size and shapes spread all over the CQD film, the SILAR samples were much smoother and practically exhibited no pits. Instead, the SILAR films exhibited cracks, formed during solvent evaporation. Both, the pits and the cracks cause light scattering and thus may act as randomly formed resonators. We attribute the differences in the film morphology of the Giant Shell samples and the SILAR samples to the different CQD shapes and eventually to a different ligand coverage. While the spherically shaped SILAR samples (see Figure S1a,b) exhibit a high tendency for self-assembly into compact arrangements with high space filling, the pyramidal shape of the Giant Shell CQDs (see Figure S1c) makes them less suitable for self-assembly. Furthermore, the AFM images showed that the microscopic film morphology varies substantially with position in the substrates. This had a major impact on the lasing thresholds, as is discussed in detail below.

Threshold dependence on film morphology. A typical feature of random lasing is a strong dependence of the laser threshold on the size of the pump spot.[43] This is caused by the increase of the return probability of the propagating light, which was scattered out of the amplification volume, with increasing excitation area. In Figure 4a the threshold intensity with respect to the

pump spot size is reported for both sample types SILAR I and Giant Shell (SILAR II is omitted in the following discussion because it essentially provides the same threshold powers as SILAR I). The measurement was performed with a stripe shaped excitation, whose length was gradually decreased and the threshold behavior measured. The theory predicts an exponential decrease of the threshold intensity for an increase of the amplification volume,[43] which is in good agreement with our results. Furthermore, we find a systematical higher threshold power for the Giant Shell sample, than for the SILAR sample. There might be several reasons for this higher threshold, which is on a first glance counterintuitive, because the Giant Shell CQDs exhibits the higher PL quantum yield as well as the longer exciton lifetime compared to SILAR CQDs. A reason for the higher threshold might be the smaller packing density of the pyramidal Giant Shell CQDs in the film or simply a slightly smaller film thickness. However, also the blue shifted XX emission with respect to the PL peak could be the origin of this higher threshold, because the biexciton emission is overlapping more with the absorption band of the single-excitons, than in the case of the type I band alignment (SILAR I). For the SILAR I sample, an outstanding low threshold intensity of 360 μJ/cm² was observed for an excitation spot size of 55 μm x 3 mm, corresponding to a power density of 185 kW/cm^2. This value represents to the best of our knowledge the lowest threshold observed for any random laser based on a CQD material (see Table S1).

As mentioned above, the surface morphology of the films plays an important role in random lasing and in fact it has an important influence on the threshold intensity. To find relations between surface morphology and lasing properties, substrates with metallic markers were used. The markers allowed adjusting of circular laser spots with a diameter of 200 μm with an accuracy of ~ 1/10 of its diameter to predefined positions on the substrates. To quantitatively compare the morphology of the film at different positions on the substrate, the samples were

inspected by dark field optical microscopy. As in the case of the gold nanostars in Figure 2c, the dark field images unraveled the features and defects in the film, that were chiefly responsible for the scattering. For the low threshold SILAR I sample, the most substantial scattering was provided by cracks in the films (Figure 5a). Film roughness also contributed to the scattered light intensity which was observed as different colored areas in between the cracks. To make these observations more quantitative, the scattered light spectrum, integrated over the whole area of the image, was measured for all positions of interest on the sample under identical conditions. The spatially integrated dark field spectra are shown in Figure 5b for the two dark field images (rectangles POS I and POS II) shown in Figure 5a. They show stray light from two contributions, (i) from the white light illumination lamp, and (ii) from the luminescence excited in the film by the lamp. The latter causes the peak at ~630 nm wavelength, while the first is seen as the background, whose intensity increases with increasing wavelength. Under laser excitation both positions shown in Figure 5a exhibit random lasing, however, with substantially different laser thresholds of 22.5 mJ/cm² and 2.7 mJ/cm², measured at POS II and POS I, respectively. Further positions on the sample provided threshold values in between these two extremes. By spectrally integrating the dark field spectra from 400 nm to 800 nm, a value for the intensity is obtained which allows ordering of the obtained threshold values. The result, shown in Figure 5c, is a systematic decrease of the laser threshold with increasing dark field intensity. Thus, film morphologies providing intense scattering are beneficial for random lasing, whereas positions were also found where no lasing could be observed. These positions appeared rather dark in the dark field images and were checked by AFM exhibit minimal surface roughness < 20 nm RMS (Figures S6)

CONCLUSION

CdSe/CdS CQDs with especially thick shells are superior compared to standard core/shell CQD materials with respect to their environmental stability and due to the possibility to control the type of their band alignment. Here three types of CdSe/CdS core/thick shell materials have been investigated – two samples fabricated with the SILAR technique and different shell thicknesses and one grown by a "Giant-Shell" method. Under pulsed laser excitation we observed amplified spontaneous emission and random lasing from biexcitons, enabled by scattering which provided the required optical feedback. Externally introduced plasmonic gold nano-particles and cracks in the films we found to act as chaotically shaped resonators providing rather stable mode patterns. Film roughness and pits caused rather random modes, which we observed as broadband, rather ASE like spectra, when they were integrated over many excitation pulses. Even though the optical feedback required for lasing was random scattering, some systematics in the threshold intensities was observed – (i) for sufficiently large excitation spots, the thresholds become insensitive to spot size and (ii) mimimal threshold are obtained for films exhibiting strong scattering. The simplicity of the random lasing experiment, performed here at room temperature and with ns long excitation pulses on films deposited on planar substrates, suggests this technique as a simple and reliable standard tool, to quantitatively evaluate CQDs for lasing purposes. Such a tool would be beneficial for materials selection and optimization, without the need of fabricating elaborate devices or of performing laborious experiments. Thus, material development for lasing purposes - various different nano-architectures such as nano-platelets, dot in rods, and nanowires are currently investigated - could be speeded up significantly, to obtain nano-lasers with continuous mode operation or also with potentially electrical excitation.

METHODS

Synthesis of SILAR CdSe/CdS CQDs. CdSe core NCs were synthesized following the established procedure described in Ref. [64]. The precursors for the alternative injections, Cd-oleate in octadecene (ODE, 0.1 M) and S-ODE (0.1M) were prepared in advance and stored under Argon. The shells of the nanocrystals were prepared according to reference [4]. A 100 mL flask was loaded with 40 mg of CdSe (3.6 nm) dissolved in 1 mL hexane, 2 ml of Oleylamine and 5 mL of ODE. The mixture was kept for 1 h under vacuum at 100 ºC. After switching to Argon, the Cd precursor was injected and the temperature was increased to 240 ºC. After 10 min. the S-precursor was injected. Every 10 min successive injections were done, to grow shells with nominal thicknesses of 8 layers (SILAR I) or 12 layers (SILAR II) of CdS. To account for the increasing diameter of NCs, the precursor volume for the first injection was 0.15 mL (0.1M concentration), 0.76 mL for the 8th layer and 1.32 mL for the 12th layer. After finishing the last injection the flask was cooled down and the NCs were washed with toluene and ethanol three times, and finally re-dispersed in 1 mL of toluene.

Synthesis of Giant Shell CdSe/CdS CQDs. Here the two-step approach reported by Chen *et al.*[8] was used with minor modification. For the synthesis of wurtzite CdSe NCs, 30 mg (0.234 mmol) CdO, 140 mg (0.418 mmol) octadecylphosphonic acid (ODPA) and 1.5 g trioctylphosphine oxide (TOPO) were mixed and degassed under Schlenk-line vacuum for 1 hour at 150 °C. Under nitrogen flow the mixture was heated up to 320°C until a clear colorless solution formed and 0.5 mL trioctylphosphine (TOP) was added. Then the reaction mixture was heated further to 370°C, the heating source was removed, and a TOPSe/TOP (30 mg Se in 0.25 mL TOP) solution was swiftly injected. Upon 10 min growth the reaction was terminated by fast cooling to room temperature. The resulting CdSe NCs were washed 3 times by acetone/hexane, redispersed in hexane and filtered through a 0.2 μm filter. The size and concentration of the NCs

were estimated by the position and amplitude of the excitonic absorption maximum, by making use of the calibration reported in Ref. [65]. For growth of the CdS shell a precursor solutions of 1.56 mmol cadmium oleate in 6 mL ODE, and 81.8 μmol hexanethiol in 6mL ODE, were prepared and degassed. The Cadmium oleate solution in ODE was prepared by heating CdO and oleic acid (1:2) in ODE up to 120°C for 1 hour. 100 nmol of CdSe NCs were mixed with 3 mL of ODE and 3 mL of oleylamine (OLA), degassed for an hour at room temperature and 15 minutes at 120°C. Under nitrogen flow the reaction solution was heated up to 310°C with the rate ~20°/min. When the temperature reached 240 °C, the slow injection of precursor solutions started with the rate of 3 mL/hour. After 2 hours 1 mL of oleic acid was injected and the solution was further annealed at 310 °C for 1 hour. The resulting NCs were washed with ethanol/hexane, re-dissolved in hexane and filtered through a 0.2 μm filter.

Synthesis of gold nanoparticles. The gold nanostars were synthesized by a seed-mediated growth and silver(I)-assisted synthesis method in aqueous solution using cetyltrimethyl ammonium bromide as the capping agent, similar as reported in[66] but using only ascorbic acid as reducing agent but no HCl, which results in a high yield of stars.

Film preparation. The CQDs were deposited on glass substrates, which were cleaned by organic solvents in an ultrasonic bath and further treated by plasma cleaning, by doctor blade casting (60°C substrate temperature). Prior to the deposition a series of markers was fabricated on the substrate, by optical lithography followed by sputtering of 50 nm Pt.

Amplified spontaneous emission measurements. For excitation, 8 ps laser pulses from a frequency doubled Nd:YAG laser (Time-Bandwidth, 532 nm, 10 kHz rep. rate), was focused by a cylindrical lens to provide a stripe on the sample. The luminescence was collected via the edge of the sample and detected by an AvaSpec-2048 spectrometer.

Random lasing experiments. Unless stated differently in the text, the samples were excited by <1.3 ns long laser pulses from a passively Q-switched solid state laser (CryLas GmbH, 532 nm, repetition rates of 100Hz and 2500Hz were used), moderately focused to a spot of ~200 μm diameter. The emission was collected in back-scattering geometry and detected by a grating spectrometer equipped with a CCD. Except explicitly stated differently, spectra which were integrated over many excitation pulses are presented in the manuscript.

Darkfield images and spectra. The dark field images were taken with an Olympus optical microscope, equipped with a camera and connected to a spectrometer. A white Anodisc 13 membrane disc was used as a reference providing uniform scattering for white light,.

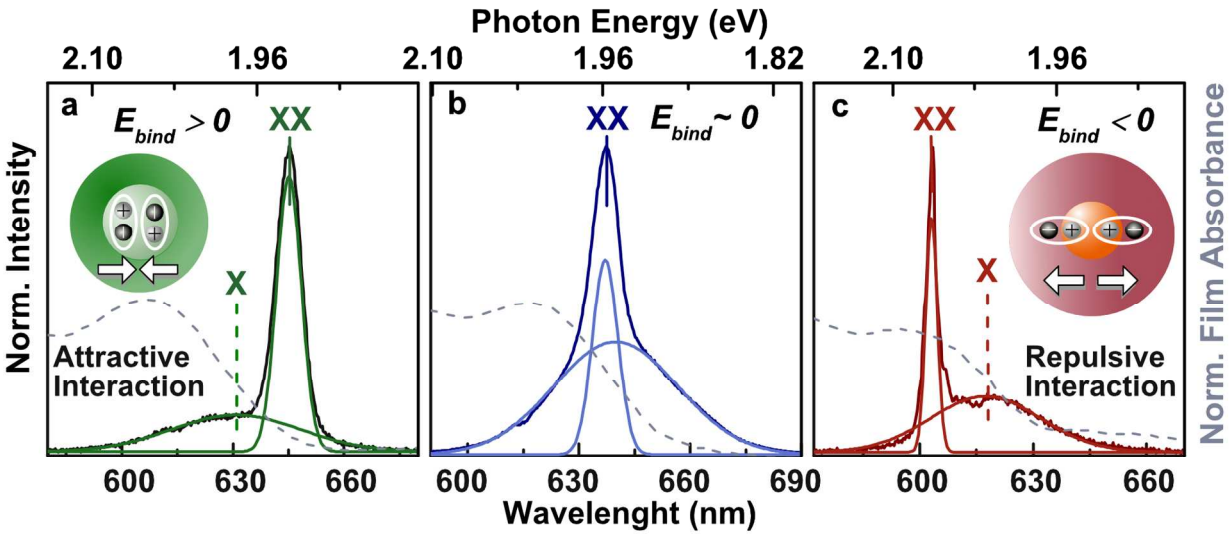

Figure 1. Amplified spontaneous emission. Under pulsed laser excitation and measured in stripe geometry, the CdSe/CdS core/thick-shell CQD films exhibit narrow emission peaks on top of the broader excitonic photoluminescence (X). The narrow peaks are caused by amplified spontaneous emission from biexcitons (XX). The wavelength shift between X and XX maxima is associated to the biexciton binding energy E_{bind}, which is (a) > 0, due to attractive exciton-exciton interactions in CQDs with type I band alignment (sample SILAR I) and (c) < 0, in type II CQDs with repulsive X-X interaction (Giant Shell sample). In (b, sample SILAR II) the exciton binding energy almost vanishes. In addition, the normalized film absorbance (grey dashed line) is presented. The 1S absorption maximum of the Giant Shell sample occurs at the ASE peak, counteracting stimulated emission.

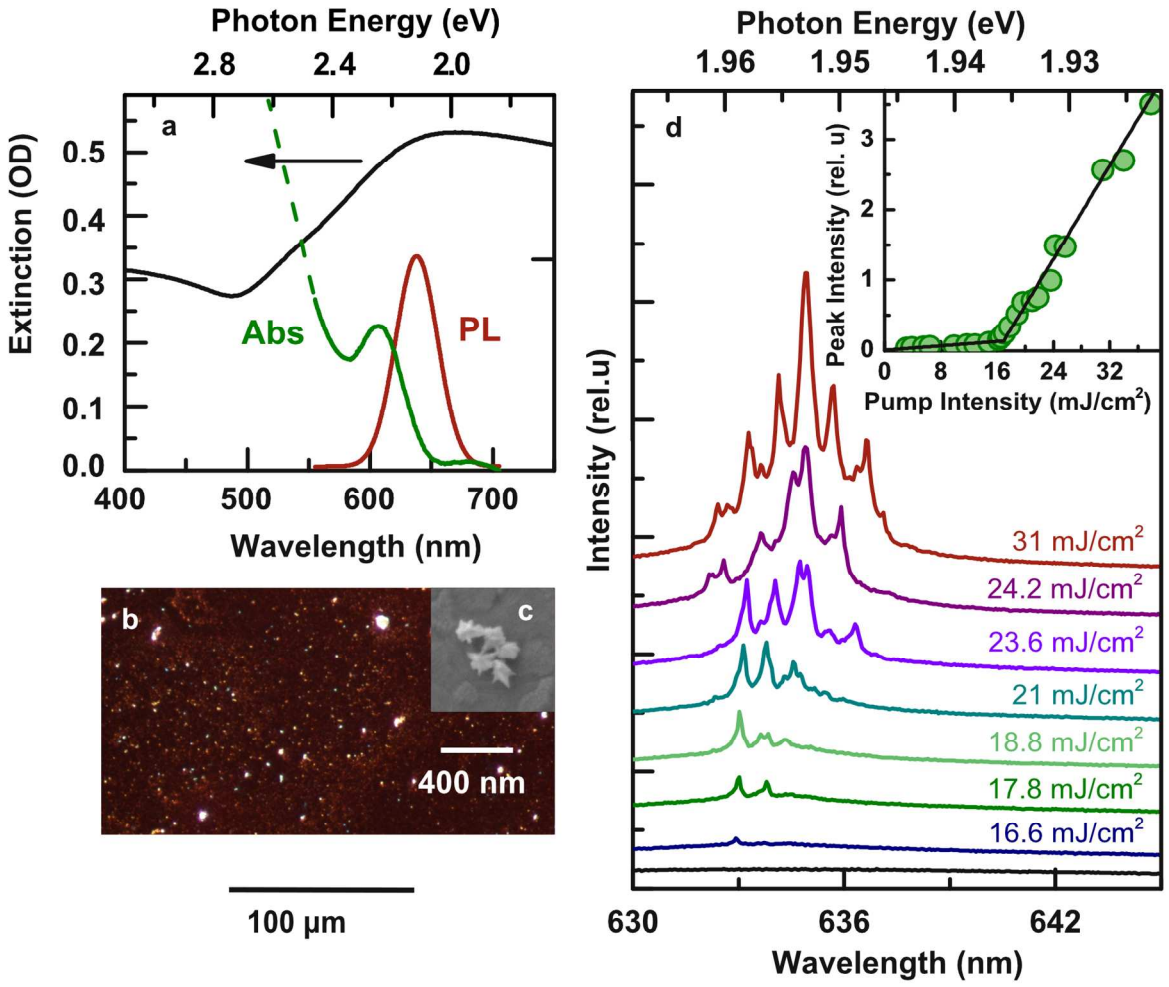

Figure 2. Random lasing due to scattering on gold nanostars. (a) The excitonic absorption peak and photoluminescence maximum of the SILAR I CdSe/CdS CQDs closely matches the extinction maximum (black line) of the plasmonic gold nanostars in solution. (b) Darkfield optical microscope image of a SILAR I CQD film on top of a glass substrate covered by gold nanostars as scattering centers. (c) Electron microscopy image of 5 plasmonic nanostars. (d) Spectral evolution of the CQD emission with increasing pump intensity and the corresponding characteristic threshold behavior, deduced from the maxima of the PL spectra (inset).

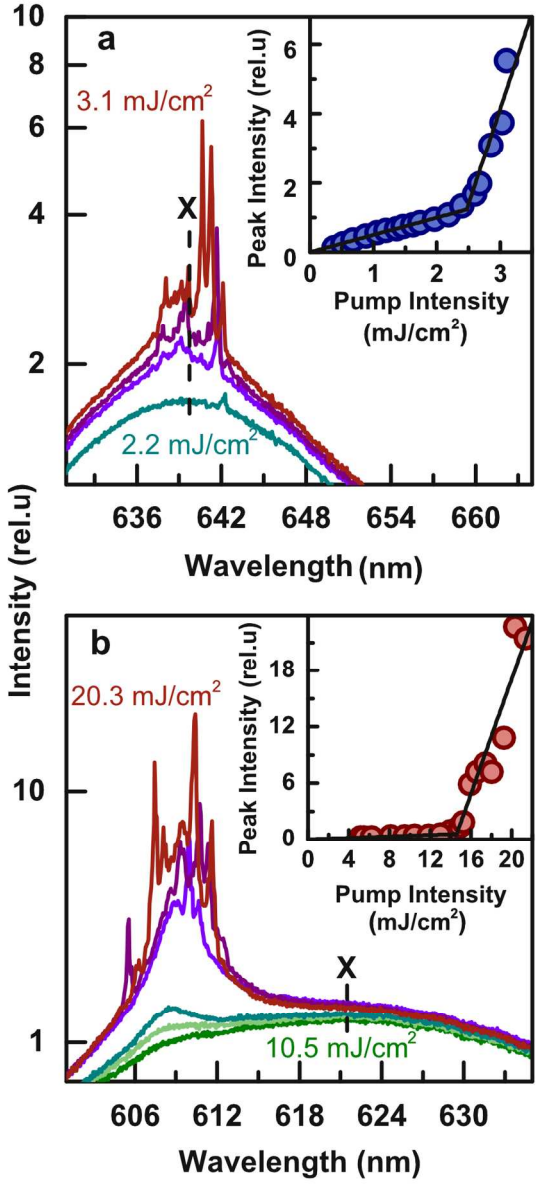

Figure 3. Random lasing with different spectral behavior. (a) SILAR II CQD films exhibit narrow laser modes just above the threshold intensity, whereas the Giant Shell film in (b) exhibits rather an amplified spontaneous emission spectrum above threshold. This different behavior points towards a different scattering mechanism to be responsible for the random lasing. Experiments are performed by < 1.3 ns laser pulses with a repetition rate of 2500 Hz. The insets present characteristic threshold curves with threshold intensities of (a) 2.2 mJ/cm² and (b) 14.5 mJ/cm², measured with a size of the excitation spot of 3.1×10^{-4} cm^2 (r=100 µm).

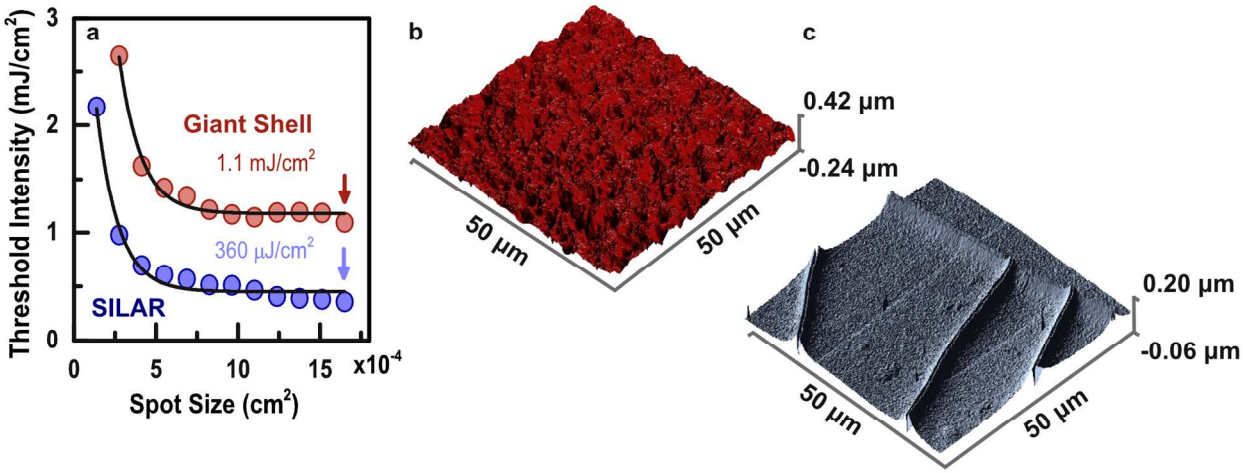

Figure 4. Threshold dependence on excitation spot size. Both sample types SILAR and Giant shell exhibit the expected exponential decrease of threshold intensity with increasing pump area (active volume). The sample providing the higher photoluminescence quantum yield (Giant Shell) exhibits the higher threshold intensity. AFM image of (b) Giant Shell sample and (c) SILAR sample, showing completely different film morphologies.

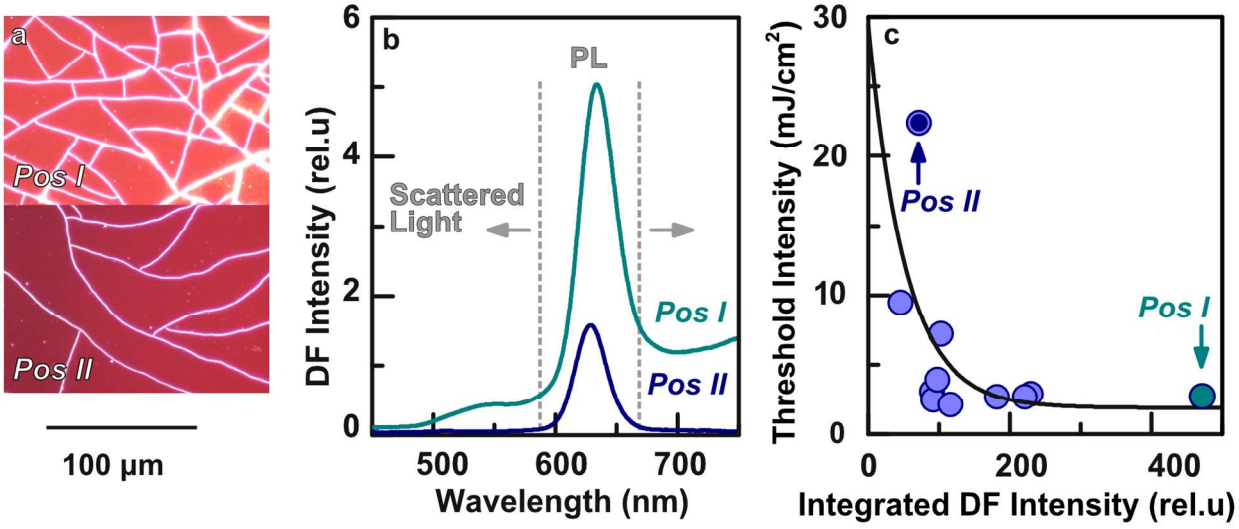

Figure 5. **Systematic dependence of threshold intensity on film morphology.** (a) Dark field optical microscopy images of two positions on a film of Silar II CQDs. Cracks contribute greatly to the scattered light intensity. Film roughness also affects scattered light and causes the films to appear in different brightness and color. (b) Spectral dependence of the scattered light, spatially integrated over the two rectangles POS I and POS II shown in (a). The peak at ˜630 nm is caused by luminescence, excited by the lamp. (c) Threshold intensity of numerous positions on the film, plotted against their corresponding spectrally integrated darkfield intensity. The laser threshold intensity decreases with increasing intensity of the scattered light. The data are fitted by an exponential decay.

ASSOCIATED CONTENT

Supporting Information. Table S1 and Supporting Figures S1 to S6. This material is available free of charge via the Internet at http://pubs.acs.org

AUTHOR INFORMATION

Corresponding Author

*Wolfgang.Heiss@fau.de

Author Contributions

The manuscript was written through contributions of all authors. All authors have given approval to the final version of the manuscript.

Funding Sources

FWF, ERC, Swiss National Science Foundation, European Union,

ACKNOWLEDGMENT

We thank the Austrian Science Fund FWF for funding through project F25 SFB-IR-ON. M.K. was funded by European Union (FP7 ERC Starting Grant 2012, GA No. 306733) and from Swiss National Science Foundation (project 200021_143638); D.D. was funded by European Union via a Marie Curie Fellowship (PIIF-GA-2012-330524). J. Z., C.V. and T. A. K. acknowledge funding by the European Research Council (ERC) via Starting Grant ‘ActiveNP’ (257158).

ABBREVIATIONS

PL photoluminescence, SILAR successive ion layer adsorption and reaction, CQDs colloidal quantum dots,

REFERENCES

1. Hines, M. A.; Guyot-Sionnest, P., Synthesis and Characterization of Strongly Luminescing ZnS-Capped CdSe Nanocrystals. *J. Phys. Chem.* **1996,** *100* (2), 468-471.
2. Peng, X.; Schlamp, M. C.; Kadavanich, A. V.; Alivisatos, A. P., Epitaxial Growth of Highly Luminescent CdSe/CdS Core/Shell Nanocrystals with Photostability and Electronic Accessibility. *JACS* **1997,** *119* (30), 7019-7029.
3. Talapin, D. V.; Rogach, A. L.; Kornowski, A.; Haase, M.; Weller, H., Highly Luminescent Monodisperse CdSe and CdSe/ZnS Nanocrystals Synthesized in a Hexadecylamine−Trioctylphosphine Oxide−Trioctylphospine Mixture. *Nano Lett.* **2001,** *1* (4), 207-211.
4. Li, J. J.; Wang, Y. A.; Guo, W.; Keay, J. C.; Mishima, T. D.; Johnson, M. B.; Peng, X., Large-Scale Synthesis of Nearly Monodisperse CdSe/CdS Core/Shell Nanocrystals Using Air-Stable Reagents via Successive Ion Layer Adsorption and Reaction. *JACS* **2003,** *125* (41), 12567-12575.
5. Reiss, P.; Bleuse, J.; Pron, A., Highly Luminescent CdSe/ZnSe Core/Shell Nanocrystals of Low Size Dispersion. *Nano Lett.* **2002,** *2* (7), 781-784.
6. Xie, R.; Kolb, U.; Li, J.; Basché, T.; Mews, A., Synthesis and Characterization of Highly Luminescent CdSe−Core CdS/Zn0.5Cd0.5S/ZnS Multishell Nanocrystals. *JACS* **2005,** *127* (20), 7480-7488.
7. Mekis, I.; Talapin, D. V.; Kornowski, A.; Haase, M.; Weller, H., One-Pot Synthesis of Highly Luminescent CdSe/CdS Core−Shell Nanocrystals via Organometallic and "Greener" Chemical Approaches†. *J. Phys. Chem. B* **2003,** *107* (30), 7454-7462.
8. Chen, O.; Zhao, J.; Chauhan, V. P.; Cui, J.; Wong, C.; Harris, D. K.; Wei, H.; Han, H.-S.; Fukumura, D.; Jain, R. K.; Bawendi, M. G., Compact high-quality CdSe–CdS core–shell nanocrystals with narrow emission linewidths and suppressed blinking. *Nat Mater* **2013,** *12* (5), 445-451.
9. Htoon, H.; Malko, A. V.; Bussian, D.; Vela, J.; Chen, Y.; Hollingsworth, J. A.; Klimov, V. I., Highly Emissive Multiexcitons in Steady-State Photoluminescence of Individual "Giant" CdSe/CdS Core/Shell Nanocrystals. *Nano Lett.* **2010,** *10* (7), 2401-2407.
10. Vela, J.; Htoon, H.; Chen, Y.; Park, Y.-S.; Ghosh, Y.; Goodwin, P. M.; Werner, J. H.; Wells, N. P.; Casson, J. L.; Hollingsworth, J. A., Effect of shell thickness and composition on blinking suppression and the blinking mechanism in 'giant' CdSe/CdS nanocrystal quantum dots. *J. Biophotonics* **2010,** *3* (10-11), 706-717.
11. Christodoulou, S.; Vaccaro, G.; Pinchetti, V.; De Donato, F.; Grim, J. Q.; Casu, A.; Genovese, A.; Vicidomini, G.; Diaspro, A.; Brovelli, S.; Manna, L.; Moreels, I., Synthesis of highly luminescent wurtzite CdSe/CdS giant-shell nanocrystals using a fast continuous injection route. *J. Mater. Chem.* **2014,** *2* (17), 3439-3447.
12. Park, Y. S.; Malko, A. V.; Vela, J.; Chen, Y.; Ghosh, Y.; García-Santamaría, F.; Hollingsworth, J. A.; Klimov, V. I.; Htoon, H., Near-Unity Quantum Yields of Biexciton Emission from CdSe\CdS Nanocrystals Measured Using Single-Particle Spectroscopy. *Phys. Rev. Lett.* **2011,** *106* (18), 187401.
13. Greytak, A. B.; Allen, P. M.; Liu, W.; Zhao, J.; Young, E. R.; Popovic, Z.; Walker, B. J.; Nocera, D. G.; Bawendi, M. G., Alternating layer addition approach to CdSe/CdS core/shell quantum dots with near-unity quantum yield and high on-time fractions. *Chem. Sci.* **2012,** *3* (6), 2028-2034.

14. Grabolle, M.; Ziegler, J.; Merkulov, A.; Nann, T.; Resch-Genger, U., Stability and Fluorescence Quantum Yield of CdSe–ZnS Quantum Dots—Influence of the Thickness of the ZnS Shell. *Ann. N. Y. Acad. Sci.* **2008,** *1130* (1), 235-241.
15. Bruchez, M.; Moronne, M.; Gin, P.; Weiss, S.; Alivisatos, A. P., Semiconductor Nanocrystals as Fluorescent Biological Labels. *Science* **1998,** *281* (5385), 2013-2016.
16. Medintz, I. L.; Uyeda, H. T.; Goldman, E. R.; Mattoussi, H., Quantum dot bioconjugates for imaging, labelling and sensing. *Nat Mater* **2005,** *4* (6), 435-446.
17. Wu, X.; Liu, H.; Liu, J.; Haley, K. N.; Treadway, J. A.; Larson, J. P.; Ge, N.; Peale, F.; Bruchez, M. P., Immunofluorescent labeling of cancer marker Her2 and other cellular targets with semiconductor quantum dots. *Nat Biotech* **2003,** *21* (1), 41-46.
18. Resch-Genger, U.; Grabolle, M.; Cavaliere-Jaricot, S.; Nitschke, R.; Nann, T., Quantum dots versus organic dyes as fluorescent labels. *Nat Meth* **2008,** *5* (9), 763-775.
19. Wolfgang, J. P.; Teresa, P.; Christian, P., Labelling of cells with quantum dots. *Nanotechnology* **2005,** *16* (2), R9.
20. Schlamp, M. C.; Peng, X.; Alivisatos, A. P., Improved efficiencies in light emitting diodes made with CdSe(CdS) core/shell type nanocrystals and a semiconducting polymer. *J. Appl. Phys.* **1997,** *82* (11), 5837-5842.
21. Sun, Q.; Wang, Y. A.; Li, L. S.; Wang, D.; Zhu, T.; Xu, J.; Yang, C.; Li, Y., Bright, multicoloured light-emitting diodes based on quantum dots. *Nat Photon* **2007,** *1* (12), 717-722.
22. Caruge, J. M.; Halpert, J. E.; Wood, V.; Bulovic, V.; Bawendi, M. G., Colloidal quantum-dot light-emitting diodes with metal-oxide charge transport layers. *Nat Photon* **2008,** *2* (4), 247-250.
23. Zhao, J.; Bardecker, J. A.; Munro, A. M.; Liu, M. S.; Niu, Y.; Ding, I. K.; Luo, J.; Chen, B.; Jen, A. K. Y.; Ginger, D. S., Efficient CdSe/CdS Quantum Dot Light-Emitting Diodes Using a Thermally Polymerized Hole Transport Layer. *Nano Lett.* **2006,** *6* (3), 463-467.
24. Pal, B. N.; Ghosh, Y.; Brovelli, S.; Laocharoensuk, R.; Klimov, V. I.; Hollingsworth, J. A.; Htoon, H., 'Giant' CdSe/CdS Core/Shell Nanocrystal Quantum Dots As Efficient Electroluminescent Materials: Strong Influence of Shell Thickness on Light-Emitting Diode Performance. *Nano Lett.* **2011,** *12* (1), 331-336.
25. Bae, W. K.; Park, Y.-S.; Lim, J.; Lee, D.; Padilha, L. A.; McDaniel, H.; Robel, I.; Lee, C.; Pietryga, J. M.; Klimov, V. I., Controlling the influence of Auger recombination on the performance of quantum-dot light-emitting diodes. *Nat Commun* **2013,** *4*.
26. Michler, P.; Imamoglu, A.; Mason, M. D.; Carson, P. J.; Strouse, G. F.; Buratto, S. K., Quantum correlation among photons from a single quantum dot at room temperature. *Nature* **2000,** *406* (6799), 968-970.
27. Fisher, B.; Caruge, J. M.; Zehnder, D.; Bawendi, M., Room-Temperature Ordered Photon Emission from Multiexciton States in Single CdSe Core-Shell Nanocrystals. *Phys. Rev. Lett.* **2005,** *94* (8), 087403.
28. Brokmann, X.; Giacobino, E.; Dahan, M.; Hermier, J. P., Highly efficient triggered emission of single photons by colloidal CdSe/ZnS nanocrystals. *Appl. Phys. Lett.* **2004,** *85* (5), 712-714.
29. Zavelani-Rossi, M.; Lupo, M. G.; Krahne, R.; Manna, L.; Lanzani, G., Lasing in self-assembled microcavities of CdSe/CdS core/shell colloidal quantum rods. *Nanoscale* **2010,** *2* (6), 931-935.

30. Grim, J. Q.; Christodoulou, S.; Di Stasio, F.; Krahne, R.; Cingolani, R.; Manna, L.; Moreels, I., Continuous-wave biexciton lasing at room temperature using solution-processed quantum wells. *Nat Nano* **2014,** *9* (11), 891-895.
31. She, C.; Fedin, I.; Dolzhnikov, D. S.; Demortière, A.; Schaller, R. D.; Pelton, M.; Talapin, D. V., Low-Threshold Stimulated Emission Using Colloidal Quantum Wells. *Nano Lett.* **2014,** *14* (5), 2772-2777.
32. Robel, I.; Gresback, R.; Kortshagen, U.; Schaller, R. D.; Klimov, V. I., Universal Size-Dependent Trend in Auger Recombination in Direct-Gap and Indirect-Gap Semiconductor Nanocrystals. *Phys. Rev. Lett.* **2009,** *102* (17), 177404.
33. Htoon, H.; Hollingsworth, J. A.; Dickerson, R.; Klimov, V. I., Effect of Zero- to One-Dimensional Transformation on Multiparticle Auger Recombination in Semiconductor Quantum Rods. *Phys. Rev. Lett.* **2003,** *91* (22), 227401.
34. Klimov, V. I.; Mikhailovsky, A. A.; McBranch, D. W.; Leatherdale, C. A.; Bawendi, M. G., Quantization of Multiparticle Auger Rates in Semiconductor Quantum Dots. *Science* **2000,** *287* (5455), 1011-1013.
35. Klimov, V. I.; Mikhailovsky, A. A.; Xu, S.; Malko, A.; Hollingsworth, J. A.; Leatherdale, C. A.; Eisler, H.-J.; Bawendi, M. G., Optical Gain and Stimulated Emission in Nanocrystal Quantum Dots. *Science* **2000,** *290* (5490), 314-317.
36. Schäfer, J.; Mondia, J. P.; Sharma, R.; Lu, Z. H.; Susha, A. S.; Rogach, A. L.; Wang, L. J., Quantum Dot Microdrop Laser. *Nano Lett.* **2008,** *8* (6), 1709-1712.
37. Min, B.; Kim, S.; Okamoto, K.; Yang, L.; Scherer, A.; Atwater, H.; Vahala, K., Ultralow threshold on-chip microcavity nanocrystal quantum dot lasers. *Appl. Phys. Lett.* **2006,** *89* (19), 191124.
38. Klimov, V. I.; Ivanov, S. A.; Nanda, J.; Achermann, M.; Bezel, I.; McGuire, J. A.; Piryatinski, A., Single-exciton optical gain in semiconductor nanocrystals. *Nature* **2007,** *447* (7143), 441-446.
39. Bachelard, N.; Gigan, S.; Noblin, X.; Sebbah, P., Adaptive pumping for spectral control of random lasers. *Nat Phys* **2014,** *10* (6), 426-431.
40. Hisch, T.; Liertzer, M.; Pogany, D.; Mintert, F.; Rotter, S., Pump-Controlled Directional Light Emission from Random Lasers. *Phys. Rev. Lett.* **2013,** *111* (2), 023902.
41. Cao, H.; Zhao, Y. G.; Ho, S. T.; Seelig, E. W.; Wang, Q. H.; Chang, R. P. H., Random Laser Action in Semiconductor Powder. *Phys. Rev. Lett.* **1999,** *82* (11), 2278-2281.
42. Cao, H.; Xu, J. Y.; Zhang, D. Z.; Chang, S. H.; Ho, S. T.; Seelig, E. W.; Liu, X.; Chang, R. P. H., Spatial Confinement of Laser Light in Active Random Media. *Phys. Rev. Lett.* **2000,** *84* (24), 5584-5587.
43. Wiersma, D. S., The physics and applications of random lasers. *Nat Phys* **2008,** *4* (5), 359-367.
44. Türeci, H. E.; Ge, L.; Rotter, S.; Stone, A. D., Strong Interactions in Multimode Random Lasers. *Science* **2008,** *320* (5876), 643-646.
45. Wiersma, D., Laser physics: The smallest random laser. *Nature* **2000,** *406* (6792), 132-135.
46. Turitsyn, S. K.; Babin, S. A.; El-Taher, A. E.; Harper, P.; Churkin, D. V.; Kablukov, S. I.; Ania-Castanon, J. D.; Karalekas, V.; Podivilov, E. V., Random distributed feedback fibre laser. *Nat Photon* **2010,** *4* (4), 231-235.
47. Wiersma, D. S.; Cavalieri, S., Light emission: A temperature-tunable random laser. *Nature* **2001,** *414* (6865), 708-709.

48. Fallert, J.; Dietz, R. J. B.; Sartor, J.; Schneider, D.; Klingshirn, C.; Kalt, H., Co-existence of strongly and weakly localized random laser modes. *Nat Photon* **2009,** *3* (5), 279-282.
49. Gottardo, S.; Sapienza, R.; Garcia, P. D.; Blanco, A.; Wiersma, D. S.; Lopez, C., Resonance-driven random lasing. *Nat Photon* **2008,** *2* (7), 429-432.
50. Redding, B.; Choma, M. A.; Cao, H., Speckle-free laser imaging using random laser illumination. *Nat Photon* **2012,** *6* (6), 355-359.
51. Tulek, A.; Polson, R. C.; Vardeny, Z. V., Naturally occurring resonators in random lasing of π-conjugated polymer films. *Nat Phys* **2010,** *6* (4), 303-310.
52. Fotiadi, A. A., Random lasers: An incoherent fibre laser. *Nat Photon* **2010,** *4* (4), 204-205.
53. Rotter, S., Random lasers: Playing pinball with light. *Nat Phys* **2014,** *10* (6), 412-413.
54. Chen, Y.; Herrnsdorf, J.; Guilhabert, B.; Zhang, Y.; Watson, I. M.; Gu, E.; Laurand, N.; Dawson, M. D., Colloidal quantum dot random laser. *Opt. Express* **2011,** *19* (4), 2996-3003.
55. Shaklee, K. L.; Leheny, R. F., DIRECT DETERMINATION OF OPTICAL GAIN IN SEMICONDUCTOR CRYSTALS. *Appl. Phys. Lett.* **1971,** *18* (11), 475-477.
56. Cihan, A. F.; Kelestemur, Y.; Guzelturk, B.; Yerli, O.; Kurum, U.; Yaglioglu, H. G.; Elmali, A.; Demir, H. V., Attractive versus Repulsive Excitonic Interactions of Colloidal Quantum Dots Control Blue- to Red-Shifting (and Non-shifting) Amplified Spontaneous Emission. *J. Phys. Chem. Lett.* **2013,** *4* (23), 4146-4152.
57. Dennis, A. M.; Mangum, B. D.; Piryatinski, A.; Park, Y.-S.; Hannah, D. C.; Casson, J. L.; Williams, D. J.; Schaller, R. D.; Htoon, H.; Hollingsworth, J. A., Suppressed Blinking and Auger Recombination in Near-Infrared Type-II InP/CdS Nanocrystal Quantum Dots. *Nano Lett.* **2012,** *12* (11), 5545-5551.
58. Dorfs, D.; Franzl, T.; Osovsky, R.; Brumer, M.; Lifshitz, E.; Klar, T. A.; Eychmüller, A., Type-I and Type-II Nanoscale Heterostructures Based on CdTe Nanocrystals: A Comparative Study. *Small* **2008,** *4* (8), 1148-1152.
59. Smith, A. M.; Mohs, A. M.; Nie, S., Tuning the optical and electronic properties of colloidal nanocrystals by lattice strain. *Nat Nano* **2009,** *4* (1), 56-63.
60. Nakamura, T.; Hosaka, T.; Adachi, S., Gold-nanoparticle-assisted random lasing from powdered GaN. *Opt. Express* **2011,** *19* (2), 467-475.
61. Popov, O.; Zilbershtein, A.; Davidov, D., Random lasing from dye-gold nanoparticles in polymer films: Enhanced gain at the surface-plasmon-resonance wavelength. *Appl. Phys. Lett.* **2006,** *89* (19), 191116.
62. Hrelescu, C.; Sau, T. K.; Rogach, A. L.; Jäckel, F.; Feldmann, J., Single gold nanostars enhance Raman scattering. *Appl. Phys. Lett.* **2009,** *94* (15), 153113.
63. van der Molen, K. L.; Tjerkstra, R. W.; Mosk, A. P.; Lagendijk, A., Spatial Extent of Random Laser Modes. *Phys. Rev. Lett.* **2007,** *98* (14), 143901.
64. Chen, O.; Chen, X.; Yang, Y.; Lynak104194h, J.; Wu, H.; Zhuang, J.; Cao, Y. C., Synthesis of Metal-Selenide Nanocrystals Using Selenium Dioxide as the Selenium Precursor. *Angewandte Chemie-International Edition* **2008,** *47* (45), 8638-8641.
65. Jasieniak, J.; Smith, L.; Embden, J. v.; Mulvaney, P.; Califano, M., Re-examination of the Size-Dependent Absorption Properties of CdSe Quantum Dots. *J. Phys. Chem. C* **2009,** *113* (45), 19468-19474.
66. Liu; Guyot-Sionnest, P., Mechanism of Silver(I)-Assisted Growth of Gold Nanorods and Bipyramids. *J. Phys. Chem. B* **2005,** *109* (47), 22192-22200.

TOC graphics

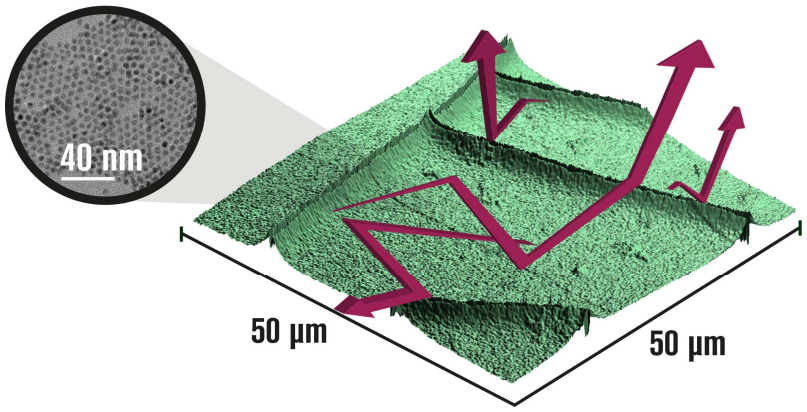

Synopsis

Films of colloidal nanocrystal quantum dots with extra thick shells operate as random lasers with relatively low threshold powers. Even though the lasing process is based on random scattering, the threshold powers show systematic dependencies. This makes the random lasing to a useful tool for a fast selection of materials for lasing purposes.